PHILOSOPHICAL TRANSACTIONS OF THE ROYAL SOCIETY A MATHEMATICAL, PHYSICAL & ENGINEERING SCIENCES

Optical Resonators Driven by Radiation Pressure

A. Dorsel, J. D. McCullen, P. Meystre, H. Walther and E. M. Wright

Phil. Trans. R. Soc. Lond. A 1984 **313**, 341-347
doi: 10.1098/rsta.1984.0116

Phil. Trans. R. Soc. Lond. A **313**, 341–347 (1984)
Printed in Great Britain

Optical resonators driven by radiation pressure

By A. Dorsel[1], J. D. McCullen[2], P. Meystre[3], H. Walther[1,3] and E. M. Wright[3]

[1] *Sektion Physik, Universität München, D-8046 Garching, Federal Republic of Germany*
[2] *Department of Physics, University of Arizona, Tucson, Arizona* 89721, *U.S.A.*
[3] *Max-Planck-Institut für Quantenoptik, D-8046 Garching, Federal Republic of Germany*

The combined effects of radiation pressure and gravitational force can be used to stabilize a moving mirror to a high degree of accuracy. A noise analysis shows that, under typical conditions, a three-mirror configuration can lead to a mirror confinement within about 1.5 nm, for incident laser powers of 0.5 W.

1. Introduction

Consider a plane Fabry–Perot interferometer in which one mirror is fixed and the other is very light, and suspended to swing as a pendulum. The light pressure produced by the intensity W_{in} in the cavity drives it towards equilibrium with the gravitational and inertial forces. At steady state, the mirror displacement x from its rest position in the absence of light is then proportional to W_{in}. Since x determines the interferometer spacing, there is a one-to-one correspondence between this situation and usual optical bistability in the presence of a Kerr medium, except that we now have a change of the physical cavity length instead of its optical length. In a previous paper (Dorsel *et al.* 1983) we showed experimentally that this system can display a bistable response (radiation-pressure optical bistability). In addition, we showed that when the incident light intensity is sufficient, the movable mirror becomes extremely stable, and the motion at the mechanical resonance is suppressed. We call this behaviour 'mirror confinement'. In view of its potential applications, efforts to analyse this control mechanism, and to exploit it further have proceeded. In particular, we found that a three-mirror device (the movable mirror is suspended between two fixed mirrors) is capable of far superior confinement and stability (McCullen *et al.* 1984). The improved stability is due to the fact that radiation pressure now acts on both sides of the movable mirror, the greater force coming from the side closest to resonance. By suitable choice of the round-trip cavity phase shift, these competing forces can be used to produce a high level of mirror confinement and stability. In §2 a review of the two-mirror system is given, and in §3 the three-mirror arrangement is discussed. A white-noise analysis of the systems is presented in §4. In §5 we discuss the effects of ground noise, which are relevant for applications, for example as a narrow-band seismometer. Finally, §6 is a summary and conclusion.

2. Two-mirror resonator

The interferometer constructed for our experimental studies has been described elsewhere (Dorsel *et al.* 1983). Bistability was obtained by slowly varying the input power across the bistable region, from feeble power to high power, and back. Scanning times ranged from 2 to 5 min, times long compared with the damping time of the mirror.

In addition to optical bistability, we also observed an effect we call mirror confinement, whereby for sufficient fixed input power the movable mirror became extremely stable against mechanically resonant oscillations at the pendulum frequency. It was found that the effective resonant frequency Ω_{eff} for the system could become significantly different from the mechanical frequency Ω of the pendulum for input power sufficiently beyond the bistability threshold.

Mirror confinement can be simply understood in terms of the potential describing the motion of the moving mirror. This potential can be derived from the dynamical equation for the moving mirror

$$\ddot{x}+\gamma\dot{x}+x = P(x), \tag{1}$$

where x measures the displacement of the mirror from its rest position in the absence of light, γ is the pendulum damping constant, and $P(x)$ is the radiation pressure force per unit mass. For scaling convenience, x is measured in units of half-wavelengths of the incident light (assumed monochromatic) and time is measured in units of the inverse of the pendulum frequency Ω. For the two-mirror system $P(x)$ is given by

$$P_2(x) = \frac{K_2}{1+F_2 \sin^2 \frac{1}{2}\phi}, \tag{2}$$

where $\phi = 2\pi x-\phi_0$, ϕ_0 being the detuning of the resonator in the absence of light. The constants K_2 and F_2 are given by

$$K_2 = \frac{4R'(1-R)\,W}{\{1-\sqrt{(RR')}\}^2\, mc\lambda\Omega^2}; \quad F_2 = \frac{4\sqrt{(RR')}}{\{1-\sqrt{(RR')}\}^2}, \tag{3}$$

where R and R' are the intensity reflectivities of the fixed and movable mirrors, respectively, W is the input intensity, and m is the movable mirror mass.

The potential corresponding to the dynamical equation (1) (we set $\gamma = 0$) is given by

$$V(x) = \tfrac{1}{2}x^2 - \int_0^x \mathrm{d}y\, P(y) \tag{4}$$

and is plotted in figure 1*a* for $R = 0.99$, $R' = 0.95$, $K_2 = 109$ (we use these values for examples throughout). This value for K_2 corresponds to an applied light power of 0.5 W, and $\Omega = 7\ \mathrm{s}^{-1}$, with a mirror mass 60 mg. The potential minima correspond to possible stable states of the system. It is clear that if the mirror is captured into one of these wells, it thereafter responds significantly only to driving forces whose frequencies are near the oscillation frequency in the well. As the input power, and thus the internal power, increases, the depth and curvature of the well increase, and the effective resonant frequency of the system departs from the pendulum frequency. For sufficient input powers the system can therefore be made extremely stable against mechanically resonant oscillations.

3. Three-mirror system

The chief drawback presented by the two-mirror system in confining the mirror is that the radiation pressure force is exerted only in one direction. Thus on one side of the equilibrium point the force changes rapidly with position (on a scale determined by the cavity finesse),

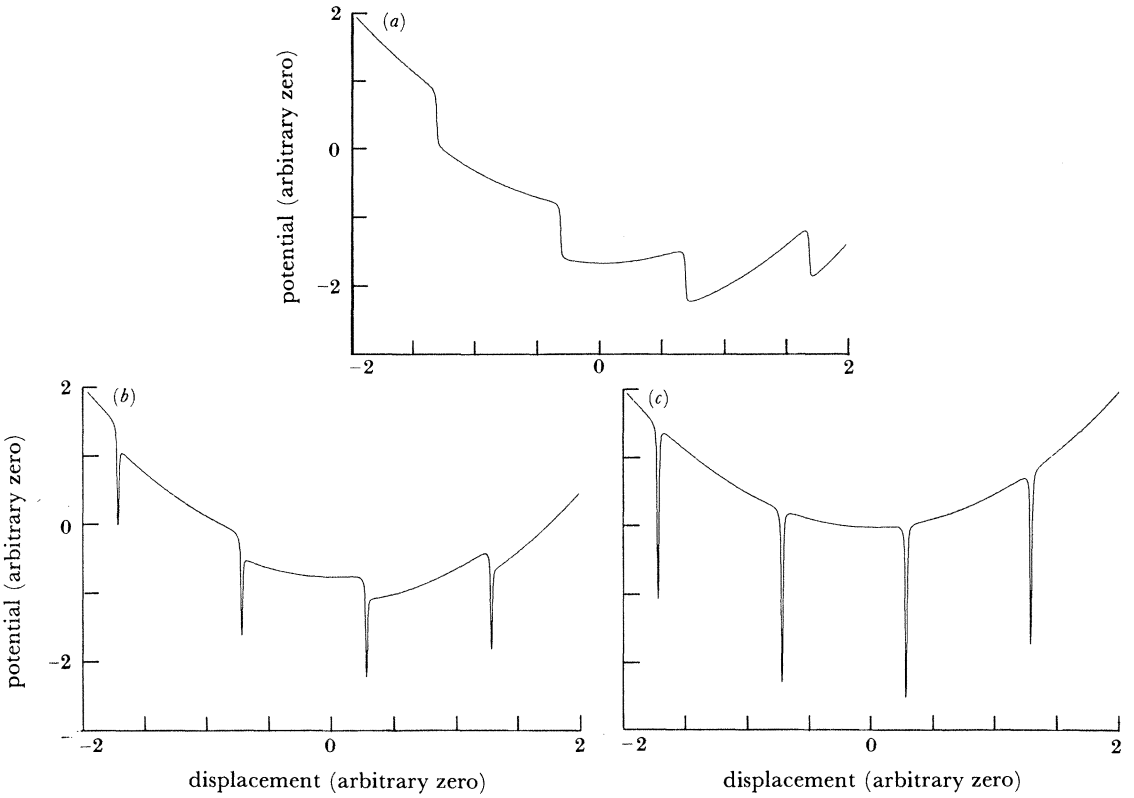

FIGURE 1. Potentials for (*a*) the two-mirror case; (*b*) the three-mirror case with one-sided illumination; (*c*) the three-mirror case with symmetric illumination, for $R = 0.99$, $R' = 0.95$, $K_2 = 109$.

whereas on the other side the restoring force comes from the usual pendulum forces, and varies much more slowly with position. The situation can be significantly improved by suspending the movable mirror inside a fixed tuned Fabry–Perot cavity, thereby creating two coupled interferometers. The radiation pressure force can now be in either direction, depending upon which of the cavities is closer to resonance, with a concomitant sharpening of its positional dependence. By appropriately tuning the main cavity, reversal of the direction of the radiation pressure occurs when the overall transmission is large, providing maximal radiation forces to confine the pendulum.

Equation (1) remains valid for the three-mirror system, but with

$$P_3 = \frac{K_3\{f(1+R) - 2\cos(\phi - \phi_1)\}}{1 + F_3\{f\cos(\phi - \tfrac{1}{2}\phi_1) - \cos\tfrac{1}{2}\phi_1\}\{fR\cos(\phi - \tfrac{1}{2}\phi_1) - \cos\tfrac{1}{2}\phi_1\}}, \tag{5}$$

where we have taken the laser field to be incident on one side of the fixed Fabry–Perot only. In this equation ϕ_1 is the (round-trip) phase detuning of the main cavity, $f = \sqrt{(R'/R)}$, and F_3 and K_3 are given by

$$F_3 = \frac{4R}{(1-R)^2}; \quad K_3 = \frac{1}{f}\left(\frac{1-fR}{1-R}\right)^2 K_2. \tag{6}$$

The denominator in (5) has a sharp minimum, similar to the denominator in (2). The value

for ϕ at which it minimizes, however, is $\sin(\phi - \frac{1}{2}\phi_1) = 0$, rather than $\sin\frac{1}{2}\phi = 0$. The value for ϕ_1 that makes this minimum the smallest is given by the equation

$$\cos\tfrac{1}{2}\phi_1 = \tfrac{1}{2}f(1+R). \tag{7}$$

With this choice of ϕ_1, the numerator of (4) passes through zero at the same value for ϕ for which the denominator minimizes. The force thus changes sign in a region of maximum transmission. Roughly speaking, this causes the equilibrium points of the mirror to occur at nodes of the standing wave of the light resonant in the main cavity.

Potential curves for the three-mirror system are plotted in figure 1*b*, *c*. Curve 1*c* is obtained with equal intensities incident on both sides of the fixed Fabry–Perot and assuming that the light beams are mutually incoherent; the force then consists of the sum of two terms, each of the form of (5):

$$P_s = 2K_3 \sin\tfrac{1}{2}\phi_1 \sin(\phi - \tfrac{1}{2}\phi_1)/D, \tag{8}$$

where D is the denominator in (5).

The curves for the three-mirror system show potential wells around equilibrium points of the movable mirror that are much narrower than their two-mirror counterparts. The examples in figure 1 are for the choice of cavity phase given by (7), which results in the narrowest wells. With ϕ_1 greater than this, the wells become deeper and the spacing between the steep walls increases, making the potential more or less flat on the bottom. For a given choice of ϕ_1, the depth of the well depends upon the intensity of the incident light. The shape, however, depends on the cavity parameters. For the case shown in figure 1, the width at half maximum is about 0.017 of the incident wavelength, or 8.5 nm with 500 nm incident light. The effective resonant frequencies for the three-mirror system can be estimated by a linearized analysis (see §5) of the dynamics represented in (1).

4. White-noise analysis

The effect of white noise on (1) can be investigated by solving the corresponding Fokker–Planck equation

$$\frac{\partial \mathscr{W}}{\partial t} = \left\{-u\frac{\partial}{\partial x} + \frac{\partial}{\partial u}\left(\gamma u + \frac{\partial V}{\partial x}\right) + \mathscr{D}\frac{\partial^2}{\partial u^2}\right\}\mathscr{W},$$

where $\mathscr{W}(x, u, t)$ is the probability density in position–velocity space and u is the movable mirror velocity in units of $u_0 = \frac{1}{2}\lambda\Omega$. $\mathscr{D} \equiv \gamma(u_{\mathrm{th}}/u_0)^2$ is the usual diffusion coefficient.

In the steady state ($\partial\mathscr{W}/\partial t = 0$) the solution of this equation is given by Risken (1984)

$$\mathscr{W}(x, u) = N \exp\left[-(u_0/u_{\mathrm{th}})^2\{\tfrac{1}{2}u^2 + V(x)\}\right], \tag{9}$$

where N is a normalization constant.

Integrating over velocities yields the probability density $Q(x)$ of finding the particle between x and $x + \mathrm{d}x$. We find

$$Q(x) = \exp\{-(u_0/u_{\mathrm{th}})^2 V(x)\} \Big/ \int_{-\infty}^{\infty} \mathrm{d}y \exp\{-(u_0/u_{\mathrm{th}})^2 V(y)\}, \tag{10}$$

which has the form of a partition function. We are interested in the confinement of the movable mirror when it is initially prepared in one of the potential minima. If this well corresponds to

essentially the same potential value as one of its close neighbours, then, according to (10), the steady-state probabilities for the mirror to be in either well will be equal. This arises because in the limit $t \to \infty$, tunnelling produces the distribution (10). However, on more realistic time scales (say hours) tunnelling will be negligible if $Q(x)$ for the initial well is narrow compared with the well width. We therefore consider individual wells and treat the remainder of the potential curve as that of the gravitational potential. In figure 2 we have plotted $Q(x)$ as a

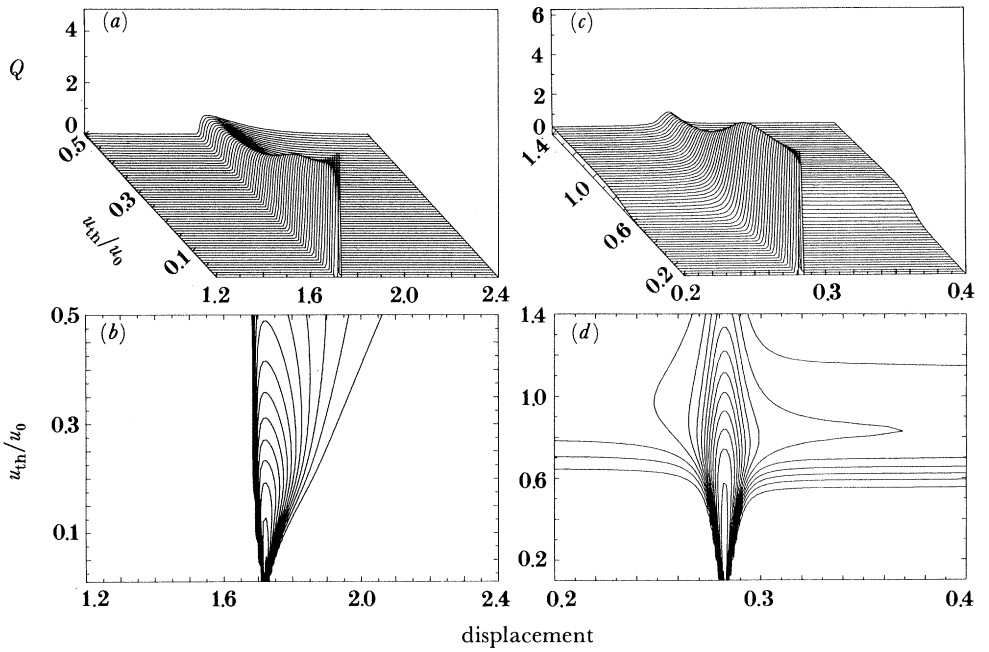

FIGURE 2. Probability density $Q(x)$ plotted against x and u_{th}/u_0 together with the corresponding contour plot for the two-mirror (a, b) and three-mirror (c, d) systems. These results correspond to the deepest potential wells in figure 1 a, b.

function of x and (u_{th}/u_0), along with a corresponding contour plot, for both the two-mirror (figure 2 a, b) and three-mirror (figure 2 c, d) cases. In each case we choose the deepest potential well (see figure 1 a, b). Figure 2 a shows that the stability of the two-mirror system to noise is somewhat limited owing to the slowly varying gravitational potential. This feature leads to fast tunnelling from the initial well to the neighbouring well on the slow side of the potential for relatively low values of u_{th}/u_0. In contrast the three-mirror system shows far superior stability to noise. Figure 2 c shows clearly that the probability density remains essentially constant in width, right up to a critical point at which the profile broadens abruptly and stability is lost. This feature is more clearly displayed in figure 2 d, where the contours diverge abruptly at $u_{th}/u_0 \approx 0.6$. For the case of two-way driving of the three-mirror system, the results are similar to those in figure 2 c, d, except that the curves are more symmetrical.

5. Effects of ground noise

The white-noise analysis of the previous section, though useful for comparing the relative stability and confinement properties of the various systems, is inappropriate to the description of ground noise, which is the main noise source as far as applications are concerned. To evaluate

its effects, we use a linearized form of (1), in which $P(x)$ is expanded to first order in x around an equilibrium point $x_0 = 0$. In the presence of ground noise source, $G(t)$, this equation becomes (x is now the displacement from the chosen equilibrium point)

$$\ddot{x} + \gamma\dot{x} + \Omega_e^2 x = G(t), \tag{11}$$

where the effective frequency Ω_e is found from

$$\Omega_e^2 = 1 + (\partial P/\partial x)_{x_0}, \tag{12}$$

which is around $\Omega_e^2 \approx 1.147 \times 10^6\ W$ for the parameters considered. This harmonic oscillator approximation is clearly most appropriate for the three-mirror systems (see figure 1*b*, *c*). If two-way pumping occurs, Ω_e^2 becomes

$$\Omega_e^2 \approx \frac{4\pi\sqrt{\{4 - f^2(1+R^2)\}}}{fT^2T'}\,W. \tag{13}$$

Assuming that the ground noise causes a translational motion $z(t)$ of the whole system through stationary air, the noise term in (11) can be written

$$G(t) = -\gamma\dot{z} - \ddot{z}. \tag{14}$$

Fourier transforming (11), for a unit impulse displacement $z(t) = \delta(t)$ yields the frequency transfer function $H(\omega)$ (Bendat & Piersol 1966),

$$H(\omega) = (\omega^2 - \mathrm{i}\gamma\omega)/(\Omega_e^2 - \omega^2 + \mathrm{i}\gamma\omega). \tag{15}$$

The spectral density $S_x(\omega)$ is then given by

$$S_x(\omega) = |H(\omega)|^2\, S_z(\omega), \tag{16}$$

where S_z is the spectral density of the ground noise, and the mean squared displacement of the moving mirror by

$$\langle x^2 \rangle = \int S_x(\omega)\, \mathrm{d}\omega. \tag{17}$$

Ground noise is characterized by a spectral density of the general form $S_z(\omega) \approx C/\omega^4$, C being a constant dependent on location. For the Munich area $C \approx 6 \times 10^{-11}/\lambda^2\Omega^3$ (Billing *et al.* 1983), the λ and Ω dependence arising from scaling. For $\lambda = 500$ nm we obtain

$$\langle x^2 \rangle \approx \frac{250}{\Omega^3} \int_{\omega_c}^{\omega_u} \frac{1}{\omega^4} \left\{ \frac{\omega^4 + \gamma^2\omega^2}{(\Omega_e^2 - \omega^2)^2 + \gamma^2\omega^2} \right\} \mathrm{d}\omega, \tag{18}$$

where ω_c is taken as a lower bound of the earth vibration frequencies, which has a value *ca.* 1 min^{-1}. In the scaled units we are using this gives $\omega_c \approx 0.1/\Omega$. The upper value, ω_u, is taken as a few times Ω_{eff}, say 10, then $\omega_u \approx 10^4\sqrt{C}$.

These values yield an x_{rms} displacement of the moving mirror of $x_{\mathrm{rms}} \approx 1.5$ nm, for $\gamma = 0.5$. With higher values of damping, x_{rms} slowly increases, because the effective resonator Q is decreased. This shows, however, that confinement to a small range of motion within the confines of the potential well is possible.

PHILOSOPHICAL TRANSACTIONS OF THE ROYAL SOCIETY A MATHEMATICAL, PHYSICAL & ENGINEERING SCIENCES

6. Summary and conclusions

Our results show that control of the position of a movable mirror to within a range of a few tenths of a nanometre by using radiation pressure, should be readily achievable. This opens the way to a number of applications, since such a system represents a very sensitive, narrow-banded tunable transducer between mechanical and optical signals. Specifically, its frequency can be tuned by varying the input laser intensity and its bandwidth by changing the phase detuning, ϕ_1, of the main cavity. For the optimal detuning ϕ_1 given by (7), a bandwidth of a few hertz can readily be achieved. Since the stabilization of the mirror is under optimum conditions about a maximum in transmission, a second, weak laser slightly detuned from the stabilizing laser should be used for detection.

Possible basic physical applications include acousto-optical studies, very accurate photoelectric effect measurements, and atomic and molecular beam diagnostics. On the more applied side, these systems can be developed into narrow-banded seismometers. An even more intriguing idea is the geometrical stabilization of a very large thin-pellicle space telescope (Labeyrie 1979).

This work was carried out partly in the framework of an operation launched by the Commission of the European Communities under the experimental phase of the European Community Stimulation Action (1983–85).

References

Bendat, J. S. & Piersol, A. G. 1966 *Measurement and analysis of random data*. New York: Wiley.
Billing, H., Winkler, W., Schilling, R., Rüdiger, A., Maischberger, K. & Schnupp, L. 1983 In *Quantum optics, experimental gravitation, and measurement theory* (ed. P. Meystre & M. O. Scully), p. 525. Plenum.
Dorsel, A., McCullen, J. D., Meystre, P., Vignes, E. & Walther, H. 1983 *Phys. Rev. Lett.* **51**, 1550.
Labeyrie, A. 1979 *Astron. Astrophys.* **77**, L1.
McCullen, J. D., Meystre, P. & Wright, E. M. 1984 *Optics Lett.* **9**, 193.
Risken, H. 1984 *The Fokker–Planck equation, methods of solutions and applications* (Springer Series in Synergetics).

PHILOSOPHICAL TRANSACTIONS OF THE ROYAL SOCIETY A MATHEMATICAL, PHYSICAL & ENGINEERING SCIENCES